HIF overexpression correlates with biallelic loss of fumarate hydratase in renal cancer: Novel role of fumarate in regulation of HIF stability

Jennifer S. Isaacs,[1,9,10] Yun Jin Jung,[6,9] David R. Mole,[7] Sunmin Lee,[2] Carlos Torres-Cabala,[1,3] Yuen-Li Chung,[8] Maria Merino,[3] Jane Trepel,[2] Berton Zbar,[4] Jorge Toro,[5] Peter J. Ratcliffe,[7] W. Marston Linehan,[1] and Len Neckers[1,*]

[1]Urologic Oncology Branch
[2]Medical Oncology Clinical Research Unit
[3]Laboratory of Pathology
[4]Laboratory of Immunobiology
[5]Genetic Epidemiology Branch
National Cancer Institute, Bethesda, Maryland 20892
[6]Laboratory of Biomedicinal Chemistry, College of Pharmacy, Pusan National University, Pusan 609-735, Korea
[7]Henry Wellcome Building for Molecular Physiology, University of Oxford, Headington, Oxford OX3 7BN, United Kingdom
[8]Cancer Research UK Biomedical Magnetic Resonance Research Group, Department of Basic Medical Sciences, St. George's Hospital Medical School, London SW17 0RE, United Kingdom
[9]These authors contributed equally to this work.
[10]Present address: Department of Cell and Molecular Pharmacology, Medical University of South Carolina, Hollings Cancer Center, 86 Jonathan Lucas Street, P.O. Box 250955, Charleston, South Carolina 29425.
*Correspondence: len@helix.nih.gov

Summary

Individuals with hemizygous germline fumarate hydratase (FH) mutations are predisposed to renal cancer. These tumors predominantly exhibit functional inactivation of the remaining wild-type allele, implicating FH inactivation as a tumor-promoting event. Hypoxia-inducible factors are expressed in many cancers and are increased in clear cell renal carcinomas. Under normoxia, the HIFs are labile due to VHL-dependent proteasomal degradation, but stabilization occurs under hypoxia due to inactivation of HIF prolyl hydroxylase (HPH), which prevents HIF hydroxylation and VHL recognition. We demonstrate that FH inhibition, together with elevated intracellular fumarate, coincides with HIF upregulation. Further, we show that fumarate acts as a competitive inhibitor of HPH. These data delineate a novel fumarate-dependent pathway for regulating HPH activity and HIF protein levels.

Introduction

Through genetic linkage analysis of afflicted families, fumarate hydratase (FH) deficiency has been implicated in the dominant hereditary syndrome hereditary leiomyomatosis renal cell carcinoma (HLRCC). Germline mutation of *FH* predisposes to cutaneous and uterine leiomyomata (smooth muscle tumors) and renal cell cancer (Kiuru et al., 2001; Launonen et al., 2001; Tomlinson et al., 2002; Toro et al., 2003). Although heterozygote carriers exhibit reduced FH enzymatic activity but are otherwise phenotypically normal, the remaining functional allele is mutated or lost in nearly all cutaneous, uterine, and renal tumors arising in these individuals (Alam et al., 2003; Tomlinson et al., 2002).

Although somatic *FH* inactivation predisposes to tumor formation, biallelic germline mutation of *FH* causes fumarate deficiency syndrome, an ultimately fatal disorder resulting in severe neurological impairment (Bourgeron et al., 1994; Gellera et al., 1990). The disparate outcome between complete and partial germline inactivation of FH function may be explained by its

SIGNIFICANCE

The inherited disorder hereditary leiomyomatosis renal cell carcinoma (HLRCC), which is characterized by germline FH mutation, is associated with cutaneous and uterine leiomyomata and renal cancer. While FH inactivation is associated with these pathologies, the causative molecular mechanisms are unknown. Herein, we demonstrate an increase in HIF and HIF-regulated transcripts in FH-inactivated and fumarate-treated cells, and we show elevated HIF protein levels in FH renal tumors. Genetic inactivation of FH and blockade of the TCA cycle necessitates a metabolic reliance upon glycolysis. Most tumor cells are dependent upon glycolysis for survival and concomitantly overexpress HIF, a transcriptional regulator of glycolysis and the hypoxic response. Fumarate-mediated HIF upregulation, coupled with inactivated FH-driven adaptation to glycolysis, together create an environment permissive for tumorigenesis.

role in metabolism. FH plays an essential role in the mitochondrial tricarboxylic acid (TCA), or Krebs cycle, by catalyzing the conversion of fumarate to malate. A primary function of the TCA cycle is the oxidation of pyruvate, supplied by the glycolytic pathway, for energy. The abrogation of FH activity has profound cellular consequences that are incompatible with normal embryologic development. Thus, the pronounced neurological defects associated with biallelic germline FH deficiency can be explained by the high energy demands of the developing nervous system during embryogenesis coupled with the dependence of neurons upon oxidative phosphorylation (Eng et al., 2003; Shulman et al., 2004).

Hypoxia-inducible factor (HIF) is a central regulator of oxygen homeostasis. HIF-1α or HIF-2α, together with HIF-1β, or ARNT, forms an active transcription complex that upregulates numerous target genes that play roles in glycolysis, angiogenesis, metastasis, and survival (for review, see Semenza, 2003). HIF gene products collectively promote adaptation to hypoxia, and HIF-1α (or in some cases HIF-2α) is overexpressed in a majority of primary tumors, cancer cell lines, and metastases (Birner et al., 2000; Talks et al., 2000; Zhong et al., 1999). HIF-1α and HIF-2α are both labile under normoxic conditions, due to proteasomal degradation following their oxygen-dependent ubiquitination by a ubiquitin ligase complex targeted to HIF by the von Hippel-Lindau (VHL) protein (Iwai et al., 1999; Maxwell et al., 1999; Ohh et al., 2000). VHL recognition of HIF requires the enzymatic hydroxylation of two conserved proline residues on HIF mediated by HIF prolyl hydroxylase (HPH) (Bruick and McKnight, 2001; Epstein et al., 2001; Ivan et al., 2001; Jaakkola et al., 2001; Yu et al., 2001). HPH activity requires the cofactors ascorbate and iron and the cosubstrates 2-oxoglutarate (2-OG) and molecular oxygen. This elegant system explains the basis for HIF stabilization under hypoxia, as HPH function and subsequently VHL recognition of hypo-hydroxylated HIF is compromised in the absence of oxygen.

Germline alteration of *VHL* is the basis for a hereditary cancer syndrome in which affected individuals are at risk to develop multiple angiogenic tumors, including clear cell renal cell carcinoma (CCRCC) (Gnarra et al., 1994; Kaelin and Maher, 1998). Almost universally, tumors arising in VHL patients or sporadic CCRCC have lost the remaining *VHL* allele (Gnarra et al., 1994; Prowse et al., 1997) and display high HIF protein levels and coincident upregulation of HIF-dependent transcripts (Iliopoulos et al., 1996; Wiesener et al., 2001). The link between HIF expression and CCRCC is further validated by the finding that reintroduction of VHL into VHL-deficient cell lines suppresses their ability to form tumors in vivo (Iliopoulos et al., 1995), an effect ascribed to reduced HIF expression (Kondo et al., 2003, 2002; Maranchie et al., 2002).

Inherited neoplastic syndromes are also associated with mutation of the succinate dehydrogenase (SDH) complex (Astuti et al., 2001; Baysal et al., 2000; Niemann and Muller, 2000), which catalyzes the conversion of succinate to fumarate in the TCA cycle. Interestingly, tumors harboring SDH mutations exhibit elevated HIF protein levels and associated hypoxia-inducible transcripts (Gimenez-Roqueplo et al., 2001), and individuals may be predisposed to early onset renal cancer (Vanharanta et al., 2004). Therefore, genetic inactivation of SDH and FH with subsequent accumulation of succinate and fumarate is correlated with cancer development, and particularly with a predisposition for renal cancer. Although a role for HIF in VHL-deficient CCRCC is well established, there are no data supporting a similar role for HIF in HLRCC tumors. In the current study, we demonstrate that HLRCC renal tumors exhibit elevated expression of HIF-1 and HIF-2 proteins, as well as the protein product of the HIF-regulated gene Glut-1. Furthermore, we show that fumarate, and to a lesser extent succinate, abrogate VHL recognition of HIF by impairing HPH activity. Finally, we demonstrate that fumarate inhibits HPH activity by competing with its cosubstrate 2-OG. These data demonstrate a direct link between fumarate dysregulation and HPH inactivation.

Results

HIF proteins are overexpressed in HLRCC renal tumors

Although a role for HIF has not been previously implicated in HLRCC renal tumors, we considered whether alteration of HIF expression is associated with these neoplasms. Tumor specimens from seven HLRCC patients were fixed and prepared for immunohistochemical analysis. Representative staining from normal and tumor tissue is shown in Figure 1. Both HIF-1 and HIF-2 proteins are uniformly overexpressed in tumor tissue. Information pertaining to germline *FH* status of these HLRCC patients has been previously reported (Toro et al., 2003; Wei et al., 2005). A summary of HIF protein expression and germline and somatic *FH* genetic status of these tumors is presented in Table 1. The majority of tumor specimens (five of seven confirmed cases) exhibited loss of heterozygosity (LOH) for *FH*, a result consistent with previous findings (Alam et al., 2003; Tomlinson et al., 2002).

FH inhibition and fumarate synergistically upregulate and stabilize HIF protein

The data in Figure 1 suggested a correlation between loss of FH and overexpression of HIF proteins in HLRCC-associated tumors. We sought to explore this relationship further on a molecular level. As there are no established HLRCC cell lines, we emulated this phenotype by exogenously adding fumarate to cultured cells in combination with 3-nitropropionic acid (3-NPA), an established dual inhibitor of SDH and FH (Coles et al., 1979; Porter and Bright, 1980). 3-NPA was used because of the lack of a specific pharmacologic inhibitor of FH. A549 cells were treated with the indicated concentration of 3-NPA and increasing concentrations of fumarate. HIF protein levels increased in a dose-dependent manner when both agents were added simultaneously, although a slight, but reproducible increase was evident with 3-NPA alone (Figure 2A). To further examine the kinetics of the fumarate-mediated HIF induction, we treated cells with 3-NPA and 2.5 mM fumarate and examined time-dependent accumulation of HIF. A modest increase in HIF protein levels was observed within 4 hr of treatment (Figure 2B, upper panel). Longer exposure of the same film (lower panel) shows that detectable upregulation of HIF occurs within 2 hr of treatment. Similar results were obtained using different esterified forms of fumarate (data not shown).

The combination of 3-NPA and fumarate did not alter the level of HIF mRNA (data not shown), suggesting that a post-transcriptional mechanism was responsible for this phenomenon. Since the α subunit of HIF is tightly regulated posttranslationally by protein degradation, we examined whether fumarate modulated HIF stability. Cells were treated as indicated (Figure 2C), and the protein synthesis inhibitor cycloheximide (CHX)

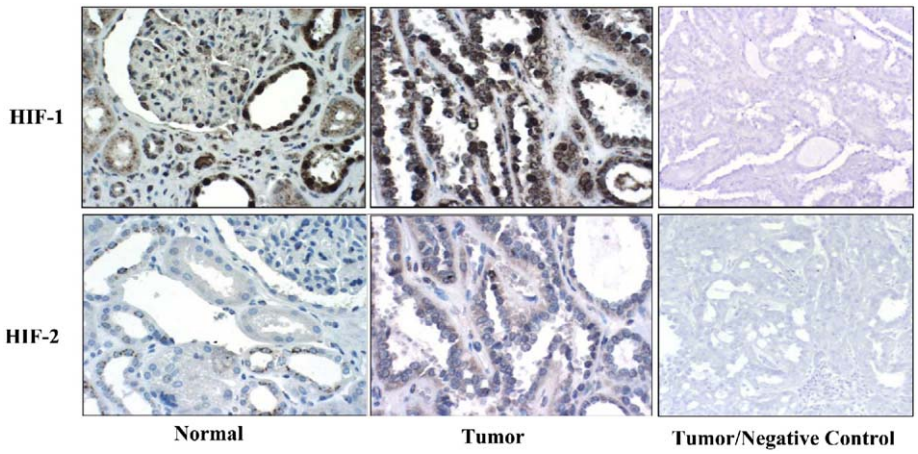

Figure 1. HIF proteins are overexpressed in FH renal tumors

Tissues were prepared for immunohistochemical detection of HIF-1 and HIF-2 proteins as described. Representative HIF staining from a HLRCC renal tumor is shown. Normal kidney tissue removed from the same patient served as a matched negative control. Antibody controls are also shown. All views are 20× magnification.

was used to determine the apparent half-life of HIF protein. In untreated cells, HIF was extremely unstable, with a half-life of 6 min. In marked contrast, 3-NPA and fumarate increased the half-life of HIF almost 5-fold to 28 min.

2-OG antagonizes fumarate- and succinate-mediated upregulation of HIF

Since 3-NPA is also a known inhibitor of SDH (Coles et al., 1979), we considered whether elevated succinate levels might affect HIF protein levels, especially in light of the finding that hereditary mutations in SDH lead to HIF-expressing paragangliomas and pheochromocytoma (Gimenez-Roqueplo et al., 2001), and a recent report that SDH siRNA promotes elevated HIF protein levels in 293 cells (Selak et al., 2005). We therefore tested whether succinate, either alone or in combination with 3-NPA, affected HIF expression in our cell model. Although succinate alone failed to increase HIF protein levels, combination of succinate and 3-NPA did weakly induce HIF, but less robustly than did 3-NPA and fumarate (Figure 3A).

Another TCA cycle intermediate, 2-OG, is an essential cosubstrate for HPH. We therefore considered whether the activity of fumarate (or succinate) could be countered by increasing the level of 2-OG. Indeed, 2-OG completely abrogated HIF-1 induction mediated either by 3-NPA and fumarate, or by high concentrations of fumarate alone (Figure 3B, left panel). Combination of fumarate and 3-NPA also induced HIF-2 in a 2-OG-sensitive manner (Figure 3B, right panel). Finally, 2-OG abrogated HIF induction caused by 3-NPA and succinate (Figure 3C), suggesting that upregulation of HIF by either succinate or fumarate impacts a pathway utilizing 2-OG.

Since 3-NPA inhibits both SDH and FH, we treated cells with siRNA specific for FH to verify that endogenous FH is involved in the 3-NPA-mediated HIF induction. Quantitative RT-PCR was used to verify siRNA-mediated downregulation of FH mRNA. FH siRNA reduced FH mRNA level in A549 cells by over 80%, while no reduction was observed with a nonspecific (NS) siRNA control (Figure 4A, upper left panel). FH siRNA reduced FH enzyme activity by more than 50% (Figure 4A, upper right panel). To confirm that FH knockdown results in increased fumarate levels, we utilized nuclear magnetic resonance (NMR) to monitor changes in intracellular fumarate, succinate, lactate, and glucose following FH siRNA (Figure 4A, lower panel). FH siRNA alone resulted in a doubling of intracellular fumarate (from 0.30 to 0.57 μmole/g protein), while addition of 5 mM exogenous fumarate (for 4 hr) to cells previously treated with FH siRNA produced a further 10-fold increase in intracellular fumarate. Neither FH siRNA alone nor the combination of FH siRNA and fumarate altered intracellular succinate, although both treatments resulted in a dramatic increase in intracellular glucose (4- to 6-fold) and lactate (60%). These data strongly suggest that loss of FH is sufficient to upregulate glycolysis. Western blotting with an antibody specific for FH confirmed a marked reduction in FH protein expression in both A549 and Caki cells following FH siRNA (Figure 4A, middle panel). Treatment of both cell lines with FH siRNA (in the absence of exogenous fumarate) induced a dose-dependent increase in HIF protein (Figure 4B, upper panel). FH siRNA also enhanced the ability of fumarate to increase HIF (Figure 4B, lower panel).

Table 1. Summary of HIF protein expression and FH mutational status in renal tumor tissue from seven HLRCC patients

Age	Sex	HIF-1α	HIF-2α	FH germline mutation	LOH 1q42
63	F	2+	1+	C823T	yes
23	M	1+	1+	C823T	NA
32	F	3+	1+	G del@1339	yes
32	M	3+	1+	A del@1162	no
24	F	1+	1+	C172T	yes
27	F	3+	0	G138+ 1C	yes
38	M	3+	1+	C568T	yes

HIF-1α and HIF-2α were quantified by immunohistochemistry, relative to normal kidney tissue. HIF staining was scored as follows: 3+, >75% cells positive; 2+, 50%–75% cells positive; 1+, 10%–50% cells positive; 0, <10% cells positive. NA, data not available.

Fumarate inhibits HIF prolyl hydroxylation by competitively inhibiting HPH

Since the activity of fumarate can be overcome by elevating the level of 2-OG, an essential cosubstrate for HPH, we next asked whether its ability to induce HIF is VHL dependent. We examined the effects of fumarate upon HIF protein levels in a VHL-deficient renal carcinoma cell line, UMRC2, and in its

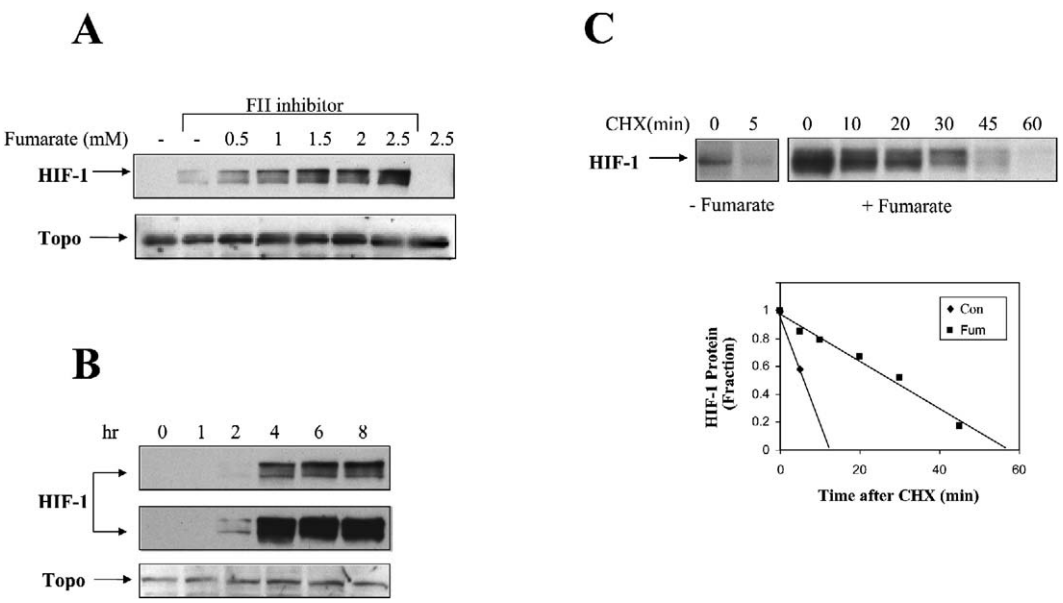

Figure 2. FH inhibition coupled with fumarate addition upregulates and stabilizes HIF protein

A: A549 lung carcinoma cells were treated for 6 hr with the FH inhibitor 3-NPA (750 μM) in combination with the indicated increasing amounts of fumarate. Nuclear extracts were probed first for HIF-1 and then for topoisomerase to confirm equal loading.

B: A549 cells were treated with the combination of 3-NPA and 2.5 mM fumarate for the indicated times. The longer exposure (bottom panel) illustrates HIF induction after a 2 hr treatment. The blot was reprobed for topoisomerase to confirm equal loading.

C: The left panel represents untreated cells and serves as a control. Right panel: A549 cells were treated as in **B** for 6 hr, whereupon CHX was added for the indicated times, and nuclear extracts were probed for HIF-1. These data are depicted quantitatively in the bottom panel.

transfected counterpart, UMRC2/VHL, which stably expresses FLAG-VHL (Isaacs et al., 2002). Combination of 3-NPA and fumarate increased HIF protein levels in UMRC2/VHL, and 2-OG antagonized this induction (Figure 5A, left panel). However, when this experiment was repeated in VHL-deficient UMRC2 cells, fumarate and 3-NPA were not able to induce HIF expression, and 2-OG was not able to diminish HIF expression (Figure 5A, right panel). To exclude any potential effects of fumarate upon VHL localization, cytoplasmic VHL expression was monitored from control or fumarate-treated cells. As shown in Figure 5A (lower left panel), there was no change in cytoplasmic VHL content in response to these treatments. Thus, these data suggest that VHL is required for both fumarate-mediated HIF induction and 2-OG-mediated HIF reduction.

We next considered whether fumarate increased HIF protein levels by interfering with HPH function. First, we examined whether fumarate reduced HPH activity in vivo. A549 cells were treated with the indicated agents, and we monitored the hydroxylation state of HIF with an antibody specific for hydroxylated HIF (Kageyama et al., 2004). The hydroxylation status of HIF was markedly reduced by 3-NPA/fumarate (Figure 5B, upper panel). As a positive control for HIF hydroxylation, cells were treated with the proteasome inhibitor PS-341 (PS lane), which permits accumulation of hydroxylated HIF, while treatment with the HPH inhibitor dimethyloxalylglycine (DMOG) served as a negative control. The lower panel of Figure 5B illustrates the total level of HIF protein following each treatment.

We then tested whether the impact of fumarate on HIF hydroxylation could be recapitulated in a cell-free system. To do so, we utilized an in vitro VHL capture assay (Tuckerman et al., 2004; Bruick and McKnight, 2001; Jaakkola et al., 2001). While the association of VHL with a HIF peptide in the absence of exogenously added HPH cofactors (control lane) is undetectable, addition of those cofactors (UT lane) markedly enhances association of HIF and VHL (Figure 5C, top panel). Strikingly, fumarate, and to a lesser degree succinate, significantly reduced this association. As we expected, 2-OG reversed the inhibitory effects of fumarate and succinate in this assay (see Figure S1 in the Supplemental Data available with this article online). Finally, we used a chemically hydroxylated peptide to verify that fumarate has a direct impact on HPH activity. Fumarate does not impair VHL association with the hydroxylated HIF peptide (Figure 5C, lower panel). Lastly, the specificity of this assay was confirmed by showing that a HIF peptide in which the two proline residues were mutated to alanine failed to bind VHL under any circumstances (data not shown).

Our data strongly support the premise that fumarate is a potent inhibitor of HPH. To determine directly whether fumarate and/or succinate inhibited HPH activity, we used purified HPH-2 (McNeill et al., 2005), the primary enzyme responsible for regulating HIF levels under normoxia (Berra et al., 2003), in a similar VHL capture assay. Because this assay uses purified enzyme, it obviates the possibility of off-pathway artifacts. Initial reaction velocities were determined at the indicated concentrations of 2-OG and fumarate, succinate, N-oxalylglycine (N-OG), or buffer alone. At high concentrations (2 mM), both fumarate and succinate inhibited HPH-2 activity (data not shown). However, dose-response curves demonstrated that fumarate more potently inhibited HPH-2 activity than did succinate (Figure 5D). From these data, the IC_{50} value for fumarate

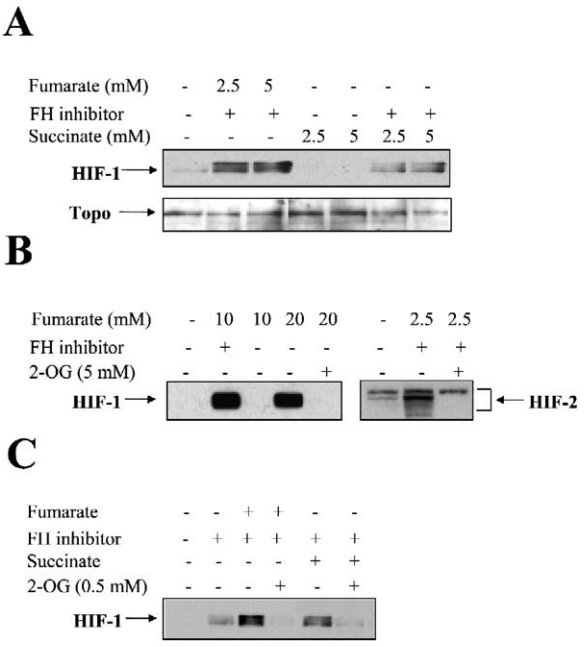

Figure 3. 2-oxoglutarate antagonizes the fumarate- and succinate-mediated upregulation of HIF

A: A549 cells were treated with 3-NPA in combination with the indicated concentrations of fumarate or succinate, and the level of nuclear HIF-1 was monitored. The blot was probed for topoisomerase to confirm equal loading.

B: Cells were treated as indicated, and the ability of exogenously added 2-oxoglutarate (2-OG) to affect the fumarate-mediated induction of HIF-1 and HIF-2 protein was assessed.

C: Cells were treated as indicated (2.5 mM fumarate or succinate, 750 μM 3-NPA), and the ability of 2-OG to affect the fumarate- or succinate-mediated induction of HIF was determined.

was determined to be 6.6 μM (±2.6), while the IC_{50} for succinate was approximately 3-fold higher, with a value of 21 μM (±8). For comparison, the ability of the HPH inhibitor N-OG (Jaakkola et al., 2001) to inhibit enzymatic activity in this assay is shown (IC_{50} = 1.3 μM).

To better assess the nature of fumarate- and succinate-mediated inhibition of HPH, we determined dose-response curves for 2-OG in the presence or absence of low concentrations of fumarate (Figure 5E, left panel) or succinate (Figure 5E, right panel). The data are illustrated as double reciprocal Lineweaver-Burke plots. The presence of either fumarate or succinate alters the apparent K_m for 2-OG (intercept with x axis) without affecting the V_{max} (intercept with y axis), indicating direct competitive inhibition with respect to 2-OG. From these data, the K_i value of fumarate was determined to be 2.6 μM (±0.2), while the K_i for succinate was approximately 3-fold higher (9 ± 0.1 μM).

Fumarate increases expression of HIF-regulated genes

Our data demonstrate that a modest (2-fold) increase in intracellular fumarate, caused by loss of FH expression, is sufficient to promote accumulation of HIF by competitively inhibiting the HPH cosubstrate 2-OG. The marked increase of intracellular glucose and lactate following FH knockdown suggested that the accumulating HIF protein is transcriptionally active and may be driving a metabolic conversion to glycolysis. To examine this question more closely, we treated A549 cells either with cobalt (a positive control), with 3-NPA/fumarate, or with FH siRNA, and we monitored the HIF-regulated transcripts Glut-1 and VEGF (Iyer et al., 1998) by quantitative RT-PCR. All treatments resulted in more than a 2-fold increase in Glut-1 mRNA (Figure 6A). These treatments also elicited an increase in VEGF mRNA, with 3-NPA/ fumarate causing the largest induction (almost 3-fold). These data are consistent with a recent report demonstrating upregulation of hypoxia-induced transcripts in FH-deficient uterine leiomyomata (Pollard et al., 2005), and they support our hypothesis that HIF protein accumulated subsequent to FH inhibition or loss is transcriptionally active.

Treatment of cells with FH siRNA elicited a small, but reproducible increase in VEGF mRNA. To validate the ability of FH siRNA to increase VEGF expression, we monitored the level of secreted VEGF protein by ELISA. siRNA treatment resulted in a modest induction of VEGF protein (2-fold and 1.8-fold, respectively) in A549 and Caki cells (Figure 6B). Although these data suggest that fumarate accumulation induces transcriptionally active HIF protein, both VEGF and Glut-1 transcripts can be induced independently from HIF (Barthel et al., 1999; Baudino et al., 2002; Okajima and Thorgeirsson, 2000). To further test whether the observed increase in these genes was HIF dependent, we used siRNA against ARNT (Isaacs et al., 2004) to reduce the levels of this essential HIF cofactor, whose dimerization with HIF is required for formation of a competent transcriptional complex (Jiang et al., 1996; Wood et al., 1996). ARNT siRNA treatment dramatically reduced ARNT protein expression in A549 cells (Figure 6C, right panel). Strikingly, treatment with ARNT siRNA reduced the basal level of Glut-1 mRNA and essentially abrogated Glut-1 induction elicited by either cobalt or 3-NPA/fumarate (Figure 6C, left panel). These data strongly suggest that fumarate-dependent elevation of Glut-1 transcripts is mediated via HIF transcriptional activity.

Finally, we wished to determine if a similar phenomenon could be demonstrated in HLRCC tumor specimens. Thus, we examined Glut-1 protein expression in three HLRCC tumor samples and three normal kidney specimens by immunohistochemistry. In the normal specimens, Glut-1 positivity was observed only in contaminating red blood cells (as expected), while strong focal staining of tumor cell membranes for Glut-1 was seen in three of three HLRCC specimens. Figure 6D depicts Glut-1 staining in a representative HLRCC and normal kidney specimen. These data highlight the significant impact of FH loss on HIF protein levels and transcriptional activity in HLRCC.

Discussion

In HLRCC, individuals are predisposed to cutaneous and uterine leiomyomata and renal cancer, yet the mechanism(s) contributing to these pathologies are unknown. We illustrate herein that HLRCC renal tumors overexpress not only HIF-1 and HIF-2 proteins, but also products of their target genes. As a result of our in vitro data, we suggest that excess intracellular fumarate, accumulating in the tumor cells in response to loss of FH, is partially responsible for this phenomenon. While it remains to be determined whether HIF upregulation is required and/or sufficient for the development of HLRCC-associated re-

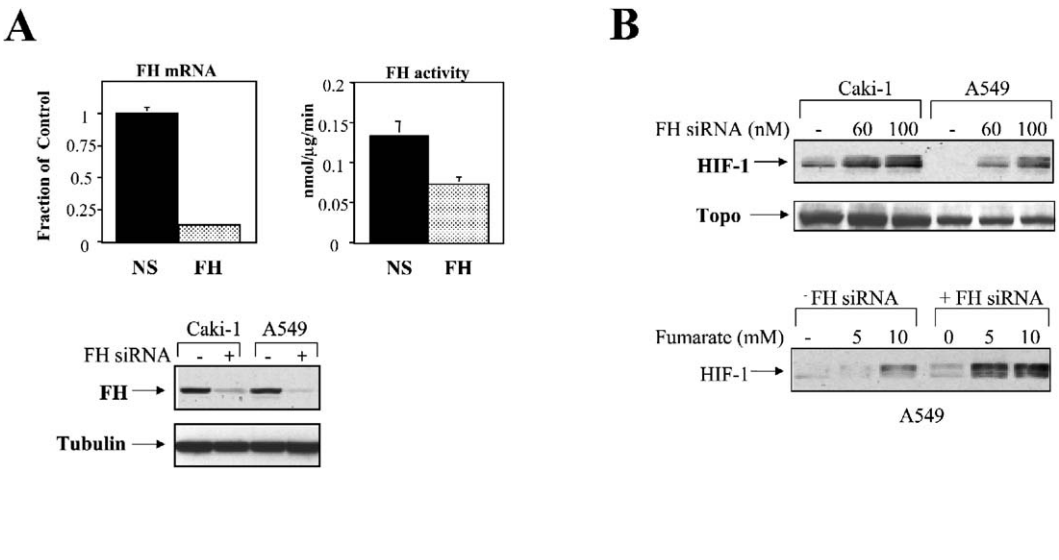

Metabolite concentration (μmole/gram protein)

	Succinate	Fumarate	Lactate	Glucose
Control	12.92	0.30	67.38	3.55
FH siRNA	14.34	0.57	112.08	20.94
FH siRNA+Fum	11.93	5.42	106.55	13.87

Figure 4. Knockdown of FH expression with siRNA induces fumarate-sensitive HIF accumulation and enhances cellular glucose uptake and lactic acid production

A: Upper left panel: RT-PCR was utilized to verify the ability of FH-siRNA to downregulate FH mRNA in A549 cells. A nonspecific (NS) siRNA served as a negative control, and message levels are represented as fraction of NS control. Upper right panel: an assay measuring endogenous FH activity was performed as described, utilizing A549 cells transfected with either NS or FH siRNA. FH activity is expressed as nmole NADPH formed/μg protein/min. Determinations for each condition were performed in triplicate, and the mean and standard error for each condition is shown. Middle panel: immunoblot analysis of FH protein level following transfection of the indicated cells with FH siRNA. Tubulin is shown for verification of equal protein loading. Bottom panel: A549 cells were either left untreated (control) or transfected on succeeding days with FH siRNA in the absence or presence of 5 mM fumarate (for 4 hr on last day). Samples were then processed for NMR analysis, and intracellular concentrations of the indicated metabolites are shown.

B: Upper panel: A549 or Caki-1 cells were transfected either with control siRNA (100 nM) or with the indicated concentrations of FH siRNA, and HIF was detected from nuclear lysates 20 hr following transfection. Lower panel: A549 cells were transfected with 60 nM FH siRNA and then treated with the indicated concentrations of fumarate the following day (for 4 hr), at which time HIF expression was determined following cell lysis.

nal cancers, we demonstrate that raising the level of intracellular fumarate upregulates VEGF and Glut-1 transcripts in a HIF-dependent manner and that HLRCC tumors express Glut-1. These data suggest that HIF expression confers a survival advantage contributing to the tumorigenic phenotype of HLRCC.

This report demonstrates a link between dysregulation of FH and modulation of HPH function. The stability and expression of HIF proteins are, in large part, regulated by the concerted actions of HPH and VHL. We clearly demonstrate that fumarate abrogates the association between HIF and VHL, due to decreased HPH-2-dependent enzymatic hydroxylation of HIF. Moreover, we present conclusive evidence that fumarate directly impairs HPH-2 function by acting as a competitive inhibitor of 2-OG. Succinate also upregulates HIF by inhibiting its proline hydroxylation (Selak et al., 2005), but in vitro enzyme kinetic analysis proves it to be a weaker antagonist of 2-OG, a finding in keeping with its reduced potency (relative to fumarate) in causing intracellular HIF accumulation in A549 cells.

Although our study emphasizes the effects of fumarate-dependent HPH inhibition on the HIF pathway, we cannot exclude the possibility that failure to degrade other, as yet undescribed HPH substrates may contribute to development of HLRCC. Indeed, the presence of a hydroxyproline binding pocket in the VHL protein (Hon et al., 2002) suggests that other VHL substrates similarly require proline hydroxylation as a prerequisite for binding to VHL. Their fate in the context of HPH inhibition remains to be examined. One must also consider the possibility that inhibition of 2-OG-dependent prolyl hydroxylation by elevated TCA cycle intermediates may favor tumorigenesis that is independent of HIF accumulation. Thus, although experimentally induced loss of SDH activity in 293 embryonal kidney cells has been shown to result in HIF accumulation via HPH inhibition (Selak et al., 2005), a more recent study in PC12 cells identifies alternative, HPH-dependent, but HIF-independent, pathways by which loss of SDH promotes tumorigenesis (Lee et al., 2005). Although the importance of HIF accumulation per se for tumorigenesis may depend on the tissue or cell type affected, endogenous levels and/or activity of HPH are generally thought to be limiting (Knowles et al., 2003), suggesting that small fluctuations in levels of either 2-OG or its competitive inhibitors could have profound effects upon HPH activity in vivo. Collectively, these recent findings highlight the potential importance of HPH in tumorigenesis.

A near-universal feature of tumor cells is their apparent reliance upon glycolysis, even under normoxia, a phenomenon termed the Warburg effect (Warburg, 1956). While the precise mechanisms underlying this metabolic shift are unclear, several lines of evidence point to HIF as a pivotal control element. HIF

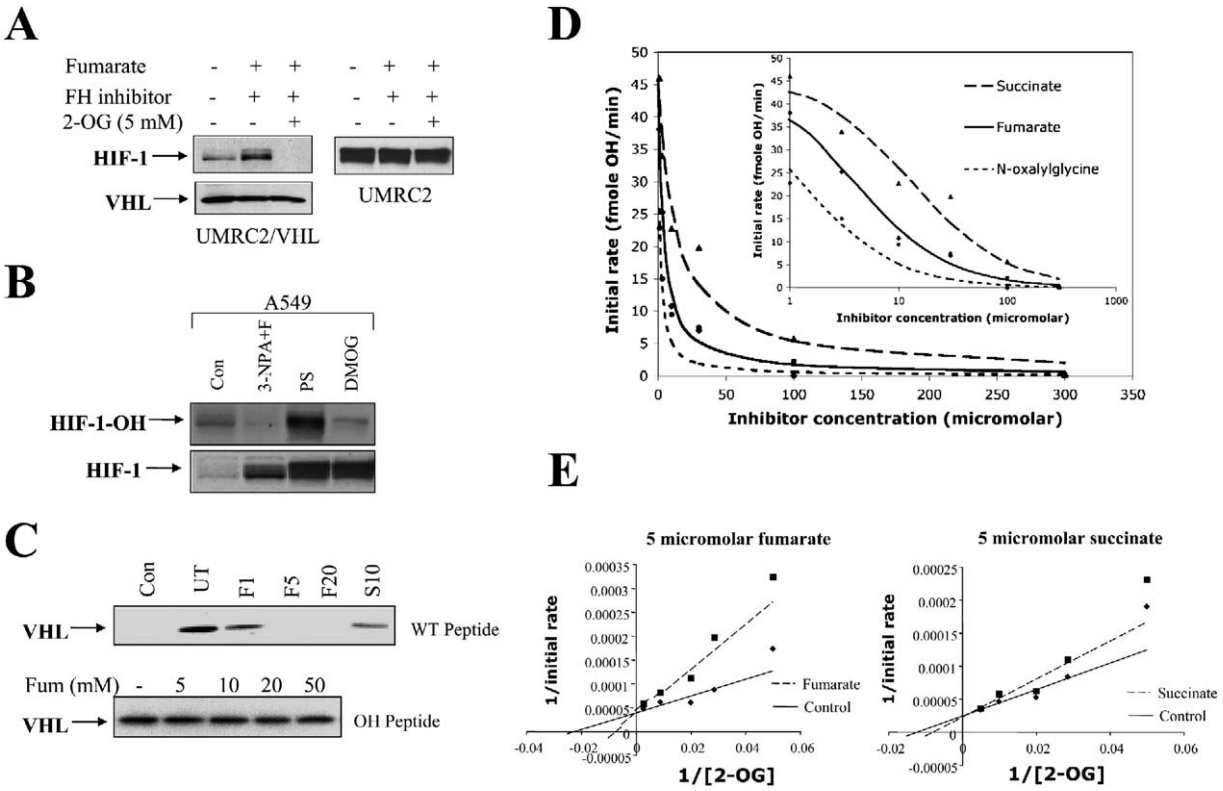

Figure 5. Fumarate upregulates HIF by inhibiting HIF prolyl hydroxylase activity

A: Parental VHL-deficient UMRC2 cells and UMRC2/VHL cells expressing stably transfected FLAG-VHL were treated as indicated, and the effects of fumarate and 2-OG upon nuclear HIF protein levels were assessed. VHL protein was immunodetected from UMRC2/VHL cytoplasmic lysates.

B: A549 cells were treated with the indicated agents and treated with proteasome inhibitor (PS) 1 hr prior to nuclear lysis as described. Resultant blots were probed with an antibody specific for hydroxylated HIF (upper panel). The lower panel demonstrates the level of nuclear HIF protein from these samples.

C: A VHL capture assay utilizing biotinylated HIF peptide was performed as described. Top panel: the assay was performed in the presence of cofactors and the indicated millimolar concentrations of fumarate (F) or succinate (S), and resultant blots were probed for FLAG (VHL). The control lane (con) represents the assay in the absence of added cofactors, while the untreated (UT) lane contains all required cofactors. Lower panel: the same assay was repeated utilizing a chemically hydroxylated peptide and increasing concentrations of fumarate.

D: Purified HPH-2 enzyme was utilized in an HPH assay as described, and the ability of either fumarate or succinate to inhibit HPH activity was assessed. The inhibitory effect of the HPH inhibitor N-oxalylglycine is shown for comparison.

E: The HPH assay was repeated with low concentrations of either fumarate (left panel) or succinate (right panel), and the inhibitory effects of these substrates upon HPH function in the presence of increasing concentrations of 2-OG were determined.

plays an essential role in sustaining glycolytic metabolism by transactivating several key substrates and enzymes of this pathway (Iyer et al., 1998; Minchenko et al., 2002; Obach et al., 2004; Ryan et al., 1998; Semenza et al., 1996). Blockade of the TCA cycle, either by hypoxia or by genetic inactivation of key enzymes such as FH and SDH, should enhance cellular reliance upon glycolysis and select for cells demonstrating upregulation of this pathway. Indeed, our data demonstrating dramatically elevated intracellular glucose and lactate levels following FH siRNA-dependent doubling of intracellular fumarate provides direct experimental evidence supporting this hypothesis. Our findings identify biallelic loss of FH as a single gene defect capable of inducing the Warburg effect. Further experimentation is needed to fully explore the link between dysregulation of the TCA cycle and tumorigenesis and to more thoroughly elucidate the roles of HIF and HPH in this process.

Experimental procedures

Cell culture and treatments

A549 and Caki-1 were obtained from the American Type Culture Collection and cultured in Dulbecco's modified Eagle's medium/F12 supplemented with 10% fetal calf serum, 2 mM glutamine, 5 mM HEPES. UMRC2 clear cell renal carcinoma cells were provided by Dr. M. Lerman (NCI, Frederick, MD). C2/VHL cells express a stably integrated VHL plasmid (Isaacs et al., 2002) and were grown in 400 μg/ml G418. Cells were treated, as indicated, with the following agents: monoethyl ester fumararic acid (MEF), 3-NPA, dimethyl 2-OG, diethyl succinate, cobalt, ascorbic acid, all purchased from Sigma. Fumarate and succinate were administered as cell-permeable esterified derivatives. DMOG and N-OG were purchased from AG Scientific, and PS-341 was from Millenium Pharmaceuticals (Cambridge, MA).

HLRCC phenotypic and genotypic assessment

Patients with suspected or confirmed HLRCC were evaluated in the Urologic Oncology Branch of the National Cancer Institute. Evaluation included history and physical examination, cutaneous examination and biopsy of cutaneous leiomyomata, abdominal and pelvic CT scan, and renal and uterine ultrasound. Three of the seven patients had renal surgery at the NCI, while the other four had surgery at outside institutions. The pathology of all of the renal tumors was reviewed by two pathologists (M.M. and C.T.-C.). Normal and tumor tissue was manually microdissected, as described (Zhuang et al., 1995), and subjected to proteinase K digestion, and DNA was extracted using the QIAamp DNA Micro Kit (QIAGEN Inc., Valencia, CA), according to the manufacturer's specifications. Sample DNA was PCR amplified using the genetic polymorphic markers D1S517, D1S2670, D1S2785, D1S304, D1S547, D1S2842, and D1S2811 (Research Genetics, Huntsville, AL) for

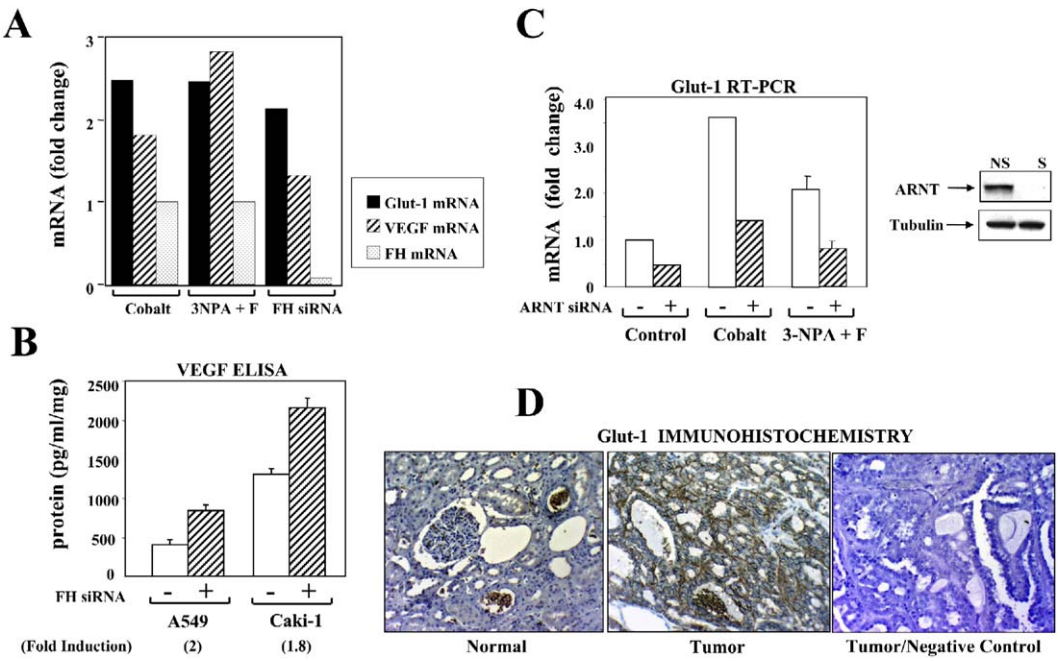

Figure 6. Fumarate increases the expression of HIF-regulated transcripts and proteins

A: A549 cells were treated as indicated, and quantitative RT-PCR was performed from total RNA utilizing primers specific for Glut-1, VEGF, or FH mRNA to determine the relative levels of message following these treatments. Values were calculated from the threshold cycle (Ct) number, as described.

B: A549 and Caki-1 were transfected with either control or FH siRNA, and secreted VEGF protein was detected from the conditioned medium by ELISA.

C: Left panel: A549 cells were transfected on successive days with either control or ARNT siRNA, and cells were treated as indicated for 8 hr in the presence or absence of ARNT siRNA. RNA was harvested, and Glut-1 message was determined utilizing RT-PCR as in **A**. The experiment was repeated three times, and mean values and standard errors are shown. Right panel: an identical set of cells was transfected, and total protein was harvested. ARNT levels were determined by immunoblot analysis, and equal protein loading was verified by tubulin protein levels.

D: Normal renal tissue and HLRCC tumor tissue were stained for Glut-1 protein by immunohistochemistry. Brown pigment reflects positive staining. In normal tissue, Glut-1 staining is only observed in red cell membranes. An antibody control is also shown.

LOH of region 1q42-44. Denatured PCR products were analyzed using the Genetic Analyzer GeneScan Analysis Program (Applied Biosystems). Each sample was processed in duplicate with negative controls, peaks corresponding to allelic expression were measured, and allelic loss was calculated. The designation of LOH was assigned to allelic imbalance values equal to or below 0.6.

Immunohistochemistry

Immunohistochemical stains were performed on formalin-fixed, paraffin-embedded tissue. Briefly, 5 mm sections were deparaffinized and rehydrated. Antigen retrieval was performed by steaming the slides in DAKO target retrieval solution (DAKO, Carpinteria, CA) for 10 min. Endogenous peroxidase activity was blocked using 3% hydrogen peroxide solution for 5 min. The antibodies and dilutions used for immunohistochemical labeling were as follows: antibodies specific for HIF-1 α (NB 100-123, clone H1α67; 1:1000) and HIF-2 α (NB 100-132, clone 190b; 1:400) were from Novus Biologicals, and polyclonal rabbit antibody to Glut-1 (A3536; 1:100) was from DAKO. Detection of immunolabeling was performed using the Catalyzed Signal Amplification system for HIF-1, and Envision Plus (both from DAKO) for HIF-2 and Glut-1, according to the manufacturer's recommendations. Diaminobenzidine was utilized as the chromogen. Negative controls, in which the primary antibody was replaced with PBS, were run with all of the samples.

Immunoblot analysis

All HIF immunoblots were performed on nuclear extracts. For subcellular fractionations, cells were washed with low-salt lysis buffer and fractionated as described (Isaacs et al., 2002). Equivalent amounts of nuclear extract were separated by 4%–20% SDS-PAGE (Bio-Rad), and the blots were subsequently probed for either HIF-1 (Transduction) or HIF-2 (Novus). For detection of hydroxylated HIF, 40 μg nuclear extract was probed with a rabbit antibody that specifically recognizes HIF hydroxylation at proline 564 (Kageyama et al., 2004). For the immunodetection of stably transfected FLAG-tagged VHL, total cell lysates were prepared as described (Isaacs et al., 2004) and probed for FLAG (Sigma). For detection of FH protein, a rabbit anti-FH antibody (Autogen Bioclear, UK) was utilized. For protein visualization, horseradish peroxidase-linked secondary antibodies were used with the ECL protein detection system (Pierce). Experiments were performed in duplicate and normalized with antibodies to topoisomerase II (nuclear extracts) or tubulin (cytoplasmic and total extracts; Sigma).

HPH-2 purification and in vitro VHL capture assay

Biotinylated wild-type or proline-hydroxylated peptides (corresponding to HIF residues 556–574) were synthesized (American Peptide Company, Sunnyvale, CA), dissolved in sterile H_2O (500 μg/ml), and incubated with streptavidin beads (Pierce ImmunoPure) at 4°C for 2 hr. The beads were washed twice with VHL binding buffer (20 mM Tris [pH 8], 100 mM NaCl, 1 mM EDTA, 0.5% NP40) and three times with reaction buffer (20 mM Tris [pH 7.5], 5 mM KCl, 1.5 mM $MgCl_2$). For each condition, 2 μg peptide/20 μl beads was aliquoted into separate tubes and reaction buffer was added, along with cofactors (500 μM α-ketoglutaric acid, 500 μM L-ascorbic acid, 50 μM ferrous chloride). Unless otherwise specified, all chemicals were purchased from Sigma. The beads and HPH cofactors were mixed at room temperature for 15 min in reaction buffer. Prior to this incubation, any inhibitors or competing factors were added to the appropriate tubes. For in vitro experiments involving fumarate or succinate competition with 2-OG, the buffered, disodium forms of these agents were used. Separate in vitro translated (IVT) reactions (Promega) were the source for the HPH protein

(HPH-2 plasmid was kindly provided S. McKnight, University of Texas Medical Center, Dallas, TX) and FLAG-VHL (Isaacs et al., 2002). A 10 μl aliquot of IVT HPH-2 was added to the bead-peptide mixture for 1 hr at 30°C. Subsequently, the beads were washed with VHL binding buffer and 10 μl FLAG-VHL IVT was added to the beads overnight at 4°C. The beads were washed, SDS Laemmli buffer was added, the samples were boiled and subjected to SDS-PAGE, and resultant blots were probed for FLAG.

As the source for purified HPH-2 protein, an N-terminally truncated HPH-2 sequence (amino acids 181–426) was subcloned into pET28a(+) and expressed in BL21(DE3), as described (McNeill et al., 2005). Purification of the His6-tagged protein was accomplished with HisBind resin (Novagen), and cleavage of the affinity tag was achieved with thrombin (Novagen). Desalting on a 300 ml Superdex-75 column (Amersham Pharmacia Biotech) yielded 95% pure protein. For the VHL capture experiments with purified HPH protein, a slightly modified protocol was used (see Supplemental Data). Reactions remained linear over the time course of the reaction, and initial reaction velocities were calculated from the slope. Calibration of peptide hydroxylation was achieved by mixing known amounts of the equivalent hydroxylated HIF-1α peptide with the nonhydroxylated peptide, thus allowing the signal obtained from captured [^{35}S]-pVHL to be calibrated against the hydroxylated peptide.

HIF half-life determination

A549 cells were treated for 6 hr with the combination of the FH inhibitor 3-NPA and fumarate. CHX was then added to the medium, and the cells were fractionated and lysed after the indicated times of CHX treatment. HIF was visualized from nuclear extracts, the films were quantitated by densitometric analysis, and the half-life was calculated using Excel.

RNA interference

Four different siRNAs corresponding to the FH coding sequence were synthesized (Qiagen), and 50–100 nM siRNA was transfected into Caki cells using previously described conditions (Isaacs et al., 2004). The next day, nuclear extracts were monitored for HIF-1 induction. The most effective FH siRNA sequence, as verified by RT-PCR (CCAGGATTATGGTCTTGAT, corresponding to residues 321–339 of FH coding sequence), was used for subsequent experiments. RNA interference for ARNT was similarly performed as previously described (Isaacs et al., 2004). A549 cells were transfected with ARNT siRNA in succession 24 hr apart, at which time the cells were treated with the indicated agents prior to RNA harvest. Control siRNA consisted of a mouse FITC-conjugated sequence (Qiagen). Control siRNA was used in each experiment in which either FH- or ARNT-specific siRNA was employed, in order to control for transfection conditions and RNA administration.

Real-time RT-PCR

RNA was isolated using the RNeasy RNA Isolation kit according to the manufacturer's instructions (Qiagen). For reverse transcription, 200 ng of total RNA was used in a reaction mixture containing 1× TaqMan RT buffer (Applied Biosystems) and Multiscribe Reverse Transcriptase. Reverse transcription was performed for 10 min at 25°C, 30 min at 48°C, and 5 min at 95°C using the PE9700 thermal cycler (Applied Biosystems). Real-time PCR primers were designed using Primer Express software (Applied Biosystems) (see Supplemental Data for information on primers and PCR conditions). The number of PCR cycles to reach the fluorescence threshold value is the cycle threshold (Ct). Ct values for the control (18S rRNA) and genes of interest were determined, and relative RNA levels were calculated by the comparative Ct method as described by the manufacturer. Experiments were performed in duplicate.

FH enzyme assay

FH activity was determined essentially as described (Hatch, 1978). Briefly, cell lysate containing a defined amount of total protein (30–100 μg) was added to a final volume of 200 μl assay buffer consisting of 25 mM HEPES-KOH (pH 7.5), 0.4 mM NADP, 4 mM $MgCl_2$, 5 mM KH_2PO_4, 0.4 units/ml NADP:malic enzyme (EC 1.1.1.4), and 10 mM fumarate. Increases in absorbance at 340 nm due to formation of NADPH were monitored at room temperature in UV-transparent 96-well flat bottom microtiter plates (Costar) in an ELx808 microplate reader (Bio-Tek). FH activity is expressed as nmole NADPH formed/μg protein/min. Samples lacking either cellular protein or fumarate were used to determine blank values.

NMR analysis of intracellular metabolites

To analyze intracellular levels of fumarate, succinate, lactate, and glucose, A549 cells were transfected with FH siRNA (100 nM) as previously described, with the modification that the cells were transfected twice in succession 24 hr apart. For each condition, six 6 cm plates were treated identically. When present, exogenous fumarate (5 mM) was added to cells for 4 hr prior to cell lysis, the day following the second transfection. The cells were washed twice with PBS and lysed in 6% cold perchloric acid. Following a 10 min centrifugation, the supernatant containing the metabolites was transferred to another tube, while the remaining protein precipitate was used for quantitation. The supernatant was neutralized with 10% potassium hydroxide, and the samples were centrifuged to remove the salt precipitate. Neutralized cell extracts were freeze dried and reconstituted in 0.6 ml deuterium oxide (Sigma, UK), 0.5 ml of which was placed in 5 mm NMR tubes. For chemical shift calibration and quantification, 50 μl of 1 mM sodium 3-trimethylsilyl-2,2,3,3-tetradeuteropropionate (Sigma, UK) was added to the samples. ^{1}H NMR spectra were obtained using a Bruker 600 MHz (Bruker Biospin, Coventry, UK) spectrometer with repetition time of 6.3 s and 384 averages. A pulse and collect with water suppression NMR sequence was used. All data were acquired under identical experimental conditions, and all shown metabolites from each sample were obtained from the same data collection. Metabolite concentrations are expressed as μmole/g total protein.

VEGF ELISA

A549 or Caki-1 cells were treated as indicated. Following transfection of FH siRNA, the medium was replaced, and the cells were allowed to incubate for 16 hr. For fumarate-treated cells, medium was collected from A549 and Caki-1 cells following 9 hr and 6 hr (respectively) of treatment. A VEGF ELISA kit (R&D Systems, MN) was used to assess secreted VEGF levels from a 200 μl aliquot of medium. Each sample was harvested for protein, which was used to normalize VEGF levels. An experiment for each condition was carried out at least once in triplicate.

Supplemental data

The Supplemental Data include Supplemental Experimental Procedures and one figure and can be found with this article online at http://www.cancercell.org/cgi/content/full/8/2/143/DC1/.

Acknowledgments

We gratefully acknowledge the efforts of Kristy Hewitson for purification of the HPH-2 enzyme. Y.-L.C. would like to thank Cancer Research UK (grant no. C12/A1212) for financial support, and the Medical Biomics Centre (St George's Hospital Medical School, London, UK) for the use of their NMR system.

Received: January 21, 2005
Revised: April 19, 2005
Accepted: June 22, 2005
Published: August 15, 2005

References

Alam, N.A., Rowan, A.J., Wortham, N.C., Pollard, P.J., Mitchell, M., Tyrer, J.P., Barclay, E., Calonje, E., Manek, S., Adams, S.J., et al. (2003). Genetic and functional analyses of FH mutations in multiple cutaneous and uterine leiomyomatosis, hereditary leiomyomatosis and renal cancer, and fumarate hydratase deficiency. Hum. Mol. Genet. *12*, 1241–1252.

Astuti, D., Latif, F., Dallol, A., Dahia, P.L., Douglas, F., George, E., Skoldberg, F., Husebye, E.S., Eng, C., and Maher, E.R. (2001). Gene mutations in the succinate dehydrogenase subunit SDHB cause susceptibility to familial pheochromocytoma and to familial paraganglioma. Am. J. Hum. Genet. *69*, 49–54.

Barthel, A., Okino, S.T., Liao, J., Nakatani, K., Li, J., Whitlock, J.P., Jr., and Roth, R.A. (1999). Regulation of GLUT1 gene transcription by the serine/threonine kinase Akt1. J. Biol. Chem. *274*, 20281–20286.

Baudino, T.A., McKay, C., Pendeville-Samain, H., Nilsson, J.A., Maclean, K.H., White, E.L., Davis, A.C., Ihle, J.N., and Cleveland, J.L. (2002). c-Myc is essential for vasculogenesis and angiogenesis during development and tumor progression. Genes Dev. *16*, 2530–2543.

Baysal, B.E., Ferrell, R.E., Willett-Brozick, J.E., Lawrence, E.C., Myssiorek, D., Bosch, A., van der Mey, A., Taschner, P.E., Rubinstein, W.S., Myers, E.N., et al. (2000). Mutations in SDHD, a mitochondrial complex II gene, in hereditary paraganglioma. Science *287*, 848–851.

Berra, E., Benizri, E., Ginouves, A., Volmat, V., Roux, D., and Pouyssegur, J. (2003). HIF prolyl-hydroxylase 2 is the key oxygen sensor setting low steady-state levels of HIF-1α in normoxia. EMBO J. *22*, 4082–4090.

Birner, P., Schindl, M., Obermair, A., Plank, C., Breitenecker, G., and Oberhuber, G. (2000). Overexpression of hypoxia-inducible factor 1α is a marker for an unfavorable prognosis in early-stage invasive cervical cancer. Cancer Res. *60*, 4693–4696.

Bourgeron, T., Chretien, D., Poggi-Bach, J., Doonan, S., Rabier, D., Letouze, P., Munnich, A., Rotig, A., Landrieu, P., and Rustin, P. (1994). Mutation of the fumarase gene in two siblings with progressive encephalopathy and fumarase deficiency. J. Clin. Invest. *93*, 2514–2518.

Bruick, R.K., and McKnight, S.L. (2001). A conserved family of prolyl-4-hydroxylases that modify HIF. Science *294*, 1337–1340.

Coles, C.J., Edmondson, D.E., and Singer, T.P. (1979). Inactivation of succinate dehydrogenase by 3-nitropropionate. J. Biol. Chem. *254*, 5161–5167.

Eng, C., Kiuru, M., Fernandez, M.J., and Aaltonen, L.A. (2003). A role for mitochondrial enzymes in inherited neoplasia and beyond. Nat. Rev. Cancer *3*, 193–202.

Epstein, A.C., Gleadle, J.M., McNeill, L.A., Hewitson, K.S., O'Rourke, J., Mole, D.R., Mukherji, M., Metzen, E., Wilson, M.I., Dhanda, A., et al. (2001). C. elegans EGL-9 and mammalian homologs define a family of dioxygenases that regulate HIF by prolyl hydroxylation. Cell *107*, 43–54.

Gellera, C., Uziel, G., Rimoldi, M., Zeviani, M., Laverda, A., Carrara, F., and DiDonato, S. (1990). Fumarase deficiency is an autosomal recessive encephalopathy affecting both the mitochondrial and the cytosolic enzymes. Neurology *40*, 495–499.

Gimenez-Roqueplo, A.P., Favier, J., Rustin, P., Mourad, J.J., Plouin, P.F., Corvol, P., Rotig, A., and Jeunemaitre, X. (2001). The R22X mutation of the SDHD gene in hereditary paraganglioma abolishes the enzymatic activity of complex II in the mitochondrial respiratory chain and activates the hypoxia pathway. Am. J. Hum. Genet. *69*, 1186–1197.

Gnarra, J.R., Tory, K., Weng, Y., Schmidt, L., Wei, M.H., Li, H., Latif, F., Liu, S., Chen, F., Duh, F.M., et al. (1994). Mutations of the VHL tumour suppressor gene in renal carcinoma. Nat. Genet. *7*, 85–90.

Hatch, M.D. (1978). A simple spectrophotometric assay for fumarate hydratase in crude tissue extracts. Anal. Biochem. *85*, 271–275.

Hon, W.C., Wilson, M.I., Harlos, K., Claridge, T.D., Schofield, C.J., Pugh, C.W., Maxwell, P.H., Ratcliffe, P.J., Stuart, D.I., and Jones, E.Y. (2002). Structural basis for the recognition of hydroxyproline in HIF-1α by pVHL. Nature *417*, 975–978.

Iliopoulos, O., Kibel, A., Gray, S., and Kaelin, W.G., Jr. (1995). Tumour suppression by the human von Hippel-Lindau gene product. Nat. Med. *1*, 822–826.

Iliopoulos, O., Levy, A.P., Jiang, C., Kaelin, W.G., Jr., and Goldberg, M.A. (1996). Negative regulation of hypoxia-inducible genes by the von Hippel-Lindau protein. Proc. Natl. Acad. Sci. USA *93*, 10595–10599.

Isaacs, J.S., Jung, Y.J., Mimnaugh, E.G., Martinez, A., Cuttitta, F., and Neckers, L.M. (2002). Hsp90 regulates a von Hippel Lindau-independent hypoxia-inducible factor-1α-degradative pathway. J. Biol. Chem. *277*, 29936–29944.

Isaacs, J.S., Jung, Y.J., and Neckers, L. (2004). Aryl hydrocarbon nuclear translocator (ARNT) promotes oxygen-independent stabilization of hypoxia-inducible factor-1α by modulating an Hsp90-dependent regulatory pathway. J. Biol. Chem. *279*, 16128–16135.

Ivan, M., Kondo, K., Yang, H., Kim, W., Valiando, J., Ohh, M., Salic, A., Asara, J.M., Lane, W.S., and Kaelin, W.G., Jr. (2001). HIFα targeted for VHL-mediated destruction by proline hydroxylation: implications for O_2 sensing. Science *292*, 464–468.

Iwai, K., Yamanaka, K., Kamura, T., Minato, N., Conaway, R.C., Conaway, J.W., Klausner, R.D., and Pause, A. (1999). Identification of the von Hippel-Lindau tumor-suppressor protein as part of an active E3 ubiquitin ligase complex. Proc. Natl. Acad. Sci. USA *96*, 12436–12441.

Iyer, N.V., Kotch, L.E., Agani, F., Leung, S.W., Laughner, E., Wenger, R.H., Gassmann, M., Gearhart, J.D., Lawler, A.M., Yu, A.Y., and Semenza, G.L. (1998). Cellular and developmental control of O_2 homeostasis by hypoxia-inducible factor 1α. Genes Dev. *12*, 149–162.

Jaakkola, P., Mole, D.R., Tian, Y.M., Wilson, M.I., Gielbert, J., Gaskell, S.J., Kriegsheim, A., Hebestreit, H.F., Mukherji, M., Schofield, C.J., et al. (2001). Targeting of HIF-α to the von Hippel-Lindau ubiquitylation complex by O_2-regulated prolyl hydroxylation. Science *292*, 468–472.

Jiang, B.H., Rue, E., Wang, G.L., Roe, R., and Semenza, G.L. (1996). Dimerization, DNA binding, and transactivation properties of hypoxia-inducible factor 1. J. Biol. Chem. *271*, 17771–17778.

Kaelin, W.G., Jr., and Maher, E.R. (1998). The VHL tumour-suppressor gene paradigm. Trends Genet. *14*, 423–426.

Kageyama, Y., Koshiji, M., To, K.K., Tian, Y.M., Ratcliffe, P.J., and Huang, L.E. (2004). Leu-574 of human HIF-1α is a molecular determinant of prolyl hydroxylation. FASEB J. *18*, 1028–1030.

Kiuru, M., Launonen, V., Hietala, M., Aittomaki, K., Vierimaa, O., Salovaara, R., Arola, J., Pukkala, E., Sistonen, P., Herva, R., and Aaltonen, L.A. (2001). Familial cutaneous leiomyomatosis is a two-hit condition associated with renal cell cancer of characteristic histopathology. Am. J. Pathol. *159*, 825–829.

Knowles, H.J., Raval, R.R., Harris, A.L., and Ratcliffe, P.J. (2003). Effect of ascorbate on the activity of hypoxia-inducible factor in cancer cells. Cancer Res. *63*, 1764–1768.

Kondo, K., Klco, J., Nakamura, E., Lechpammer, M., and Kaelin, W.G., Jr. (2002). Inhibition of HIF is necessary for tumor suppression by the von Hippel-Lindau protein. Cancer Cell *1*, 237–246.

Kondo, K., Kim, W.Y., Lechpammer, M., and Kaelin, W.G., Jr. (2003). Inhibition of HIF2α is sufficient to suppress pVHL-defective tumor growth. PLoS Biol. *1*, e83. 10.1371/journal.pbio.0000083

Launonen, V., Vierimaa, O., Kiuru, M., Isola, J., Roth, S., Pukkala, E., Sistonen, P., Herva, R., and Aaltonen, L.A. (2001). Inherited susceptibility to uterine leiomyomas and renal cell cancer. Proc. Natl. Acad. Sci. USA *98*, 3387–3392.

Lee, S., Nakamura, E., Yang, H., Wei, W., Linggi, M.S., Sajan, M.P., Farese, R.V., Freeman, R.S., Carter, B.D., Kaelin, W.G., Jr., and Schlisio, S. (2005). Neuronal apoptosis linked to EglN3 prolyl hydroxylase and familial pheochromocytoma genes: Developmental culling and cancer. Cancer Cell *8*, this issue, 155–167.

Maranchie, J.K., Vasselli, J.R., Riss, J., Bonifacino, J.S., Linehan, W.M., and Klausner, R.D. (2002). The contribution of VHL substrate binding and HIF1-α to the phenotype of VHL loss in renal cell carcinoma. Cancer Cell *1*, 247–255.

Maxwell, P.H., Wiesener, M.S., Chang, G.W., Clifford, S.C., Vaux, E.C., Cockman, M.E., Wykoff, C.C., Pugh, C.W., Maher, E.R., and Ratcliffe, P.J. (1999). The tumour suppressor protein VHL targets hypoxia-inducible factors for oxygen-dependent proteolysis. Nature *399*, 271–275.

McNeill, L.A., Bethge, L., Hewitson, K.S., and Schofield, C.J. (2005). A fluorescence-based assay for 2-oxoglutarate-dependent oxygenases. Anal. Biochem. *336*, 125–131.

Minchenko, A., Leshchinsky, I., Opentanova, I., Sang, N., Srinivas, V., Armstead, V., and Caro, J. (2002). Hypoxia-inducible factor-1-mediated expression of the 6-phosphofructo-2-kinase/fructose-2,6-bisphosphatase-3 (PFKFB3) gene. Its possible role in the Warburg effect. J. Biol. Chem. *277*, 6183–6187.

Niemann, S., and Muller, U. (2000). Mutations in SDHC cause autosomal dominant paraganglioma, type 3. Nat. Genet. *26*, 268–270.

Obach, M., Navarro-Sabate, A., Caro, J., Kong, X., Duran, J., Gomez, M., Perales, J.C., Ventura, F., Rosa, J.L., and Bartrons, R. (2004). 6-Phosphofructo-2-kinase (pfkfb3) gene promoter contains hypoxia-inducible factor-1 binding sites necessary for transactivation in response to hypoxia. J. Biol. Chem. *279*, 53562–53570.

Ohh, M., Park, C.W., Ivan, M., Hoffman, M.A., Kim, T.Y., Huang, L.E., Pavletich, N., Chau, V., and Kaelin, W.G. (2000). Ubiquitination of hypoxia-inducible factor requires direct binding to the β-domain of the von Hippel-Lindau protein. Nat. Cell Biol. *2*, 423–427.

Okajima, E., and Thorgeirsson, U.P. (2000). Different regulation of vascular endothelial growth factor expression by the ERK and p38 kinase pathways in v-ras, v-raf, and v-myc transformed cells. Biochem. Biophys. Res. Commun. *270*, 108–111.

Pollard, P., Wortham, N., Barclay, E., Alam, A., Elia, G., Manek, S., Poulsom, R., and Tomlinson, I. (2005). Evidence of increased microvessel density and activation of the hypoxia pathway in tumours from the hereditary leiomyomatosis and renal cell cancer syndrome. J. Pathol. *205*, 41–49.

Porter, D.J., and Bright, H.J. (1980). 3-carbanionic substrate analogues bind very tightly to fumarase and aspartase. J. Biol. Chem. *255*, 4772–4780.

Prowse, A.H., Webster, A.R., Richards, F.M., Richard, S., Olschwang, S., Resche, F., Affara, N.A., and Maher, E.R. (1997). Somatic inactivation of the VHL gene in von Hippel-Lindau disease tumors. Am. J. Hum. Genet. *60*, 765–771.

Ryan, H.E., Lo, J., and Johnson, R.S. (1998). HIF-1α is required for solid tumor formation and embryonic vascularization. EMBO J. *17*, 3005–3015.

Selak, M.A., Armour, S.M., Mackenzie, E.D., Boulahbel, H., Watson, D.G., Mansfield, K.D., Pan, Y., Simon, M.C., Thompson, C.B., and Gottlieb, E. (2005). Succinate links TCA cycle dysfunction to oncogenesis by inhibiting HIF-α prolyl hydroxylase. Cancer Cell *7*, 77–85.

Semenza, G.L. (2003). Targeting HIF-1 for cancer therapy. Nat. Rev. Cancer *3*, 721–732.

Semenza, G.L., Jiang, B.H., Leung, S.W., Passantino, R., Concordet, J.P., Maire, P., and Giallongo, A. (1996). Hypoxia response elements in the aldolase A, enolase 1, and lactate dehydrogenase A gene promoters contain essential binding sites for hypoxia-inducible factor 1. J. Biol. Chem. *271*, 32529–32537.

Shulman, R.G., Rothman, D.L., Behar, K.L., and Hyder, F. (2004). Energetic basis of brain activity: implications for neuroimaging. Trends Neurosci. *27*, 489–495.

Talks, K.L., Turley, H., Gatter, K.C., Maxwell, P.H., Pugh, C.W., Ratcliffe, P.J., and Harris, A.L. (2000). The expression and distribution of the hypoxia-inducible factors HIF-1α and HIF-2α in normal human tissues, cancers, and tumor-associated macrophages. Am. J. Pathol. *157*, 411–421.

Tomlinson, I.P., Alam, N.A., Rowan, A.J., Barclay, E., Jaeger, E.E., Kelsell, D., Leigh, I., Gorman, P., Lamlum, H., Rahman, S., et al. (2002). Germline mutations in FH predispose to dominantly inherited uterine fibroids, skin leiomyomata and papillary renal cell cancer. Nat. Genet. *30*, 406–410.

Toro, J.R., Nickerson, M.L., Wei, M.H., Warren, M.B., Glenn, G.M., Turner, M.L., Stewart, L., Duray, P., Tourre, O., Sharma, N., et al. (2003). Mutations in the fumarate hydratase gene cause hereditary leiomyomatosis and renal cell cancer in families in North America. Am. J. Hum. Genet. *73*, 95–106.

Tuckerman, J.R., Zhao, Y., Hewitson, K.S., Tian, Y.M., Pugh, C.W., Ratcliffe, P.J., and Mole, D.R. (2004). Determination and comparison of specific activity of the HIF-prolyl hydroxylases. FEBS Lett. *576*, 145–150.

Vanharanta, S., Buchta, M., McWhinney, S.R., Virta, S.K., Peczkowska, M., Morrison, C.D., Lehtonen, R., Januszewicz, A., Jarvinen, H., Juhola, M., et al. (2004). Early-onset renal cell carcinoma as a novel extraparaganglial component of SDHB-associated heritable paraganglioma. Am. J. Hum. Genet. *74*, 153–159.

Warburg, O. (1956). On the origin of cancer cells. Science *123*, 309–314.

Wei, M.H., Toure, O., Glenn, G., Pithukpakorn, M., Stolle, C., Choyke, P., Grubb, R., Middleton, L., Turner, M.L., Neckers, L., et al. (2005). Novel mutations in FH and expansion of the spectrum of phenotypes expressed in families with hereditary leiomyomatosis and renal cell cancer. J. Med. Genet., in press. Published online June 10, 2005. 10.1136/jmg.2005.033506.

Wiesener, M.S., Munchenhagen, P.M., Berger, I., Morgan, N.V., Roigas, J., Schwiertz, A., Jurgensen, J.S., Gruber, G., Maxwell, P.H., Loning, S.A., et al. (2001). Constitutive activation of hypoxia-inducible genes related to overexpression of hypoxia-inducible factor-1α in clear cell renal carcinomas. Cancer Res. *61*, 5215–5222.

Wood, S.M., Gleadle, J.M., Pugh, C.W., Hankinson, O., and Ratcliffe, P.J. (1996). The role of the aryl hydrocarbon receptor nuclear translocator (ARNT) in hypoxic induction of gene expression. Studies in ARNT-deficient cells. J. Biol. Chem. *271*, 15117–15123.

Yu, F., White, S.B., Zhao, Q., and Lee, F.S. (2001). HIF-1α binding to VHL is regulated by stimulus-sensitive proline hydroxylation. Proc. Natl. Acad. Sci. USA *98*, 9630–9635.

Zhong, H., De Marzo, A.M., Laughner, E., Lim, M., Hilton, D.A., Zagzag, D., Buechler, P., Isaacs, W.B., Semenza, G.L., and Simons, J.W. (1999). Overexpression of hypoxia-inducible factor 1α in common human cancers and their metastases. Cancer Res. *59*, 5830–5835.

Zhuang, Z., Bertheau, P., Emmert-Buck, M.R., Liotta, L.A., Gnarra, J., Linehan, W.M., and Lubensky, I.A. (1995). A microdissection technique for archival DNA analysis of specific cell populations in lesions < 1 mm in size. Am. J. Pathol. *146*, 620–625.